

Non-monotonic and distinct temperature responses of soil microbial functional groups of different origins and in different soils

Zhongkui Luo¹, Zuoxin Tang², Xiaowei Guo², Jiang Jiang², and Osbert Sun³

¹Zhejiang University - Zijingang Campus

²Affiliation not available

³Beijing Forestry University

May 5, 2020

Abstract

The fate of soil carbon (C) under climatic warming predominantly depends on temperature sensitivity of soil microbial functioning, but it is poorly understood. Using temporal measurements of soil respiration in an incubation experiment with cross-inoculation of microbial communities to contrasting soils, we constrained a microbial-explicit C model to infer temperature responses of two general microbial functional groups: fast-growing r- vs slow-growing K-strategists. We found that the two groups exhibit distinct, non-monotonic temperature responses. Both historical environment, under which the microbial communities were originated, and current environment, under which the microbial communities are colonized/adapted, significantly shape the temperature responses of the two groups. Our findings highlight the importance of combined effects of historical and current environment on microbial decomposition for regulating soil C dynamics under warming. We suggest that distinct, non-monotonic temperature responses of microbial functional groups may cause pronounced feedbacks between soil C dynamics and warming depending on climate-soil-microbe interactions.

Introduction

Soil carbon (C) cycling is primarily driven by microbial communities which use soil organic matter as energy sources and replenish soil C pool via microbial debris (Bardgett *et al.* 2008; McGuire & Treseder 2010; Schimel & Schaeffer 2012; Crowther *et al.* 2019). As microbial metabolism is inherently a temperature-dependent process, a great number of studies have tried to detect changes in soil microbial metabolic properties (e.g., substrate use efficiency and enzyme activities) under warming conditions and then derive relationships of these changes with soil C dynamics (Allison *et al.* 2010; Frey *et al.* 2013; Wieder *et al.* 2013). Yet, a mechanistic relationship of microbial respiration with temperature and microbial functional properties is difficult to be established (Karhu *et al.* 2014; Carey *et al.* 2016; Walker *et al.* 2018), due to challenges in accurately measuring microbial functional properties, high spatiotemporal variability of microbial community and activity, and confounding environmental constraints *in situ*. To better predict soil C dynamics under climate change, especially warming, an explicit understanding of microbial mechanisms underpinning variations of temperature sensitivity of microbial decomposition with environmental conditions (e.g., temperature, substrate availability and soil physiochemical properties) is needed.

Microbial decomposition of soil organic materials is an integrated consequence of a series of microbial processes such as C use efficiency, enzyme activity, growth and mortality. It is reasonable to expect that temperature responses of microbial decomposition may strongly depend on how individual microbial functional properties respond to warming as well as on their combined responses. We hypothesize that microbial functional properties such as growth efficiency and enzyme activity exhibit distinct temperature responses (Karhu *et al.* 2014; Walker *et al.* 2018; Min *et al.* 2019). Indeed, by conducting a meta-analysis synthesizing global datasets, Chen *et al.* (2018) found that activities of cellulase and ligninase enzymes exert

different responses to temperate changes, resulting in shift of soil C composition and alteration of overall vulnerability of soil C as a cohort to climatic warming. We postulate that this kind of differential responses are common for other microbial functional properties, and the specific response is nonlinear and strongly depend on local climate and soil conditions. For a typical microbial functional property, we assume that its temperature response can be monotonic or non-monotonic (Fig. 1). A monotonic response defines that microbial functional property preserves consistent positive or negative responses to temperature (Fig. 1a and b), while a non-monotonic response suggests the existence of turning point(s) with inverse response at the two sides of the turning point (Fig. 1c and d). In systems with different climate, soil, vegetation and/or management conditions, we further assume that the temperature responses of microbial properties among systems can be parallel or nonparallel (Fig. 1). Parallel and nonparallel responses define that the response of the microbial functional property to temperature exhibits the same pattern among soils (Fig. 1a and c) and is soil-dependent (Fig. 1b and d), respectively.

We used a data-model integration approach to test our hypotheses. Process-based microbial C models are a powerful tool to understand key microbial processes governing soil C cycling, because they are usually equipped with equations explicitly simulating microbial growth, enzyme activity, respiration, death, substrate use efficiency etc., which are otherwise difficult, if not impossible, to measure in situ but are key parameters determining soil C turnover. If these parameters are properly constrained using observational data under well-designed experiments, microbial-explicit models can provide valuable insights into detailed microbial processes. In this study, we used experimental data from a fully reciprocal incubation experiment (Tang *et al.* 2018) to constrain the model. The experimental data involved reciprocal transplant of microbial inoculums to three sterilized soils from three contrasting forest ecosystems. The incubation was conducted at three temperatures (5, 15 and 25 °C) for 61 days, capturing several critical phases of microbial growth from initial exponential increase due to microbial colonization of the sterilized soil, to rapid decrease due to depletion of preferential SOC substrates, to a relative stable state. This dataset provides a good opportunity to test whether the microbial model can capture these distinct phases, and to assess whether and how microbial community structure (which is represented by three microbial inoculum origins), soil physiochemical environment (which is represented by three sterilized soils from different climate zones), temperature and their interactions influence microbial functional properties.

Materials and Methods

Data sources

The measurements of microbial respiration from a fully reciprocal incubation experiment we recently published (Tang *et al.* 2018) were used in this study. In brief, the incubation was conducted as a full factorial design consisting of three sterilized soils (which were collected from the 0–10 cm mineral soil layer in cool temperate, warm temperate, and subtropical forests, respectively), three microbial inoculums (which were originated from the three soils), and three incubation temperatures (5, 15, and 25°C) under a constant soil moisture of 50% of soil water holding capacity, with five replicates. Before incubation, soils were treated with autoclaving (121°C, 45 min) twice in succession and again 24 h later for complete sterilization. Then, the sterilized soil was pre-incubated for 4 days at the designated temperatures (5, 15, and 25°C) to confirm the effectiveness of sterilization. After confirming the sterilization, the microbial inoculum was introduced into the sterilized soil, and then the soil was incubated for another 61 days to enable microbial community to grow and stabilize. During the 61-day incubation period, microbial respiration rates (i.e., CO₂ efflux from the incubated soil at the unit of $\mu\text{g CO}_2\text{-C g}^{-1}\text{ SOC day}^{-1}$) were measured on day 0, 1, 2, 4, 6, 9, 13, 19, 32, 39, 45, 52 and 61. Microbial biomass C was measured at the start and end of the experiment. The standard deviation (σ) and mean (μ) of the five replicates at each measurement were used to construct the probability distribution function (PDF) for microbial respiration rates assuming normality. The PDF was used to quantify uncertainties in model simulations induced by measurement uncertainty (see data assimilation section).

A microbial carbon model

We developed a microbial model to simulate microbial respiration and biomass. In the model, SOC is divided into labile (SOC_l , which is readily available for microbes) and recalcitrant pools (SOC_r , which has to be depolymerized or degraded by microbial extracellular enzymes before it can be assimilated). Microbes are the engine of the transformation of the two C pools and are divided into two functional groups, namely r-strategists (M_r) and K-strategists (i.e., M_K). A detailed description about the rationale of modeling two microbial functional groups can be found in Wieder *et al.* (2014, 2015). Microbial processes considered in the model include uptake/assimilation of SOC_l by microbes and death of microbes. The two microbial groups were simulated using Michaelis-Menten equation:

$$\frac{dM}{dt} = MGE \bullet V_{max,U} \bullet M \bullet \frac{SOC_l}{K_U + SOC_l} - \tau \bullet M, \quad (1)$$

where MGE is the microbial growth efficiency, $V_{max,U}$ the maximum microbial uptake rate of SOC_l , K_U the corresponding half-saturation constant for the uptake, and τ the death rate of M . The change of SOC_l and SOC_r can be respectively written as:

$$\frac{dSOC_l}{dt} = f \bullet \tau \bullet M + V_{max,ED} \bullet SOC_r \bullet \frac{M}{K_{ED} + M} - V_{max,U} \bullet M \bullet \frac{SOC_l}{K_U + SOC_l}, \quad (2)$$

$$\frac{dSOC_r}{dt} = (1 - f) \bullet \tau \bullet M - V_{max,ED} \bullet SOC_r \bullet \frac{M}{K_{ED} + M}, \quad (3)$$

where f is the fraction of dead microbes contributing to SOC_l , while the remaining fraction $1 - f$ contributes to SOC_r . The model simulates extracellular enzyme degradation of SOC_r using reverse Michaelis-Menten equation (Ahrens *et al.* 2015), and $V_{max,ED}$ is the maximum degradation rate by extracellular enzymes excreted by microbes, and K_{ED} the corresponding half-saturation constant of microbial biomass for the degradation. In the model, microbial respiration (MR) is the only source of CO_2 efflux, and calculated as the difference between total C uptake and that used for microbial growth:

$$\frac{dMR}{dt} = (1 - MGE) \bullet V_{max,U} \bullet M \bullet \frac{SOC_l}{K_U + SOC_l}. \quad (4)$$

Data assimilation with the microbial model

We run the model at daily time step and was constrained to capture the observed time courses of microbial respiration ($\mu g CO_2-C g^{-1} SOC day^{-1}$) and microbial biomass (μg microbial biomass $C g^{-1}$ soil C) using the Nelder-Mead algorithm which allows linear inequality constraints of model parameters (Lange, 2010). The sum of the probability density of predictions (θ , i.e., the objective function of the algorithm) was maximized to target the best agreement between model predictions and observations for each of the 27 treatments (i.e., 3 temperatures \times 3 soil types \times 3 microbial inoculums), taking into account the uncertainty in measurements:

$$\theta = \sum_{i=1}^n \frac{1}{\sqrt{2 \bullet \pi \bullet \sigma_i^2}} \bullet e^{-\frac{(x_i - \mu_i)^2}{2 \bullet \sigma_i^2}}, \quad (5)$$

where μ_i is the mean of i^{th} observations (i.e., the mean of the PDF of the measurements), σ_i the standard deviation of i^{th} observations (i.e., the standard deviation of the PDF of the measurements), x_i the corresponding model predictions, n the total sample size of observations including microbial respiration and biomass. The optimization was repeated 200 times independently, generating 200 ensembles representing the parameters' posterior distributions and including uncertainties induced by variation in observations and by parameter equifinality (Luo *et al.* 2015, 2017). Focusing on seven microbial-related parameters (i.e., $V_{max,U}$, $V_{max,ED}$, K_U , K_{ED} , τ , f , and MGE , Table 1), then, we estimated their means and 95% confidence interval

through 5,000 bootstrapped samples of the 200 estimates. If the 95% CIs of a parameter under different treatments do not overlap, the treatments were considered having significant effect on that parameter.

For the initial pool size of labile C (i.e., SOC_1), we assumed a prior uniform distribution ranging from 0 to 10% of measured initial total SOC content (microbial biomass was considered separately) at the beginning of the experiment (SOC_0 , which is different among the three soils), given that $\text{SOC}_1 + \text{SOC}_r = \text{SOC}_0$. In a specific soil, SOC_1 and SOC_r at the start of the experiment were assumed to keep the same for all temperature and microbial inoculum treatments, since temperature and microbial inoculums cannot change initial sizes of SOC pools. For the initial pool size of M_r and M_K , the sum of them was assigned to the measured total microbial biomass C in microbial inoculums, while the proportional composition of M_r and M_K was optimized. We generated prior uniform distributions for model parameters, acknowledging different growth strategies of microbial functional groups, i.e., fast-growing r- (M_r) and slow-growing K-strategists (M_K) (Weider *et al.* 2014, 2015, and references therein). Specifically, $V_{max,U}$ was assumed to range from 0 (i.e., no C assimilated by microbes) to 10 day^{-1} (ten times of microbial biomass C), with a precondition that $V_{max,U(r)} > V_{max,U(K)}$ (hereafter, we use a subscript to indicate microbial functional groups, i.e., r and K for r- and K-strategists respectively). K_U was assumed to range from 0 (i.e., microbial C assimilation is not limited by substrate availability) to the initial pool size, with a precondition that $K_{U(r)} > K_{U(K)}$. $V_{max,ED}$ was assumed to range from 0 (i.e., no degradation) to 1 day^{-1} (100% degradation of SOC_r), with a precondition that $V_{max,U(r)} < V_{max,U(K)}$. K_{ED} was assumed to range from 0 (i.e., extracellular degradation is not limited by microbial biomass) to the initial microbial pool size, with a precondition that $K_{ED(r)} < K_{ED(K)}$. τ was assumed to range from 0 (no microbial death) to 1 day^{-1} (100% microbial death), with a precondition of $\tau_r > \tau_K$, while MGE was assumed to range from 0.1 to 0.8, with a precondition of $\text{MGE}_r < \text{MGE}_K$.

Simulation experiments using the optimized model

Using the optimized model, we conducted a modeling experiment to further demonstrate the consequences of microbial origin, soil type and temperature (which were reflected by optimized model parameters under the 27 microbial origin by soil type by temperature combinations) on soil microbial respiration. To do so, the optimized model was re-run for 61 days with a constant C input rate of $100 \mu\text{g C g}^{-1}\text{soil C day}^{-1}$ for all soils under all microbial inoculums and temperatures. Cumulative microbial respiration during the 61-day simulation was calculated for each of the 27 microbial origin by soil type by temperature combinations. The difference of cumulative microbial respiration between simulations with and without C input was calculated, and compared among the 27 combinations, with its average and 95% confidence interval were estimated based on simulations using the 200 optimized parameter ensembles. This comparison enables us to assess that how microbes of different origins and in different soils respond to C input under different temperatures.

Results

Pooling all data together, the optimized microbial model could explain 92% and 93% of the variances in observed microbial respiration (MR, Fig. 2a) and biomass carbon (MB, Fig. 2b), respectively. Fig. 3 shows an example demonstrating that the temporal dynamics of MR, including an exponential increase in MR until reaching a peak and a gradual decline to a relatively stable state, can be well captured by the model. Different parameter ensembles taking into account measurement uncertainty could equally-well simulate MR, due to parameter equifinality. This example also highlighted that microbial communities originated from different soils exhibit quite different temporal dynamics of respiration (e.g., the peak respiration rate) though inoculated into the same soil under the same temperature (Fig. 3a vs 3c vs 3e). Microbial biomass C could also be captured by the model (Fig. 3b, d, and f). However, because of the availability of only two measurements at the start and end of the experiment, the model predicted great uncertainties over the experimental duration.

For most microbial-related parameters, the responses to temperature were non-monotonic and non-parallel (Fig. 1d), depending on microbial and soil origins (Fig. 4). This was true for both r- and K- strategists (Fig. 4). For example, the death rate (τ) of K-strategists decreased when temperature increased from 5 to 15 °C,

but increased when temperature increased from 15 to 25 °C, in all soils using the same microbial inoculum from Dinghu soil (i.e., non-monotonic); MGE, microbial growth efficiency, showed the similar pattern (Fig. 4). $V_{\max, U}$, the maximum C uptake rate by microbes, showed inverse responses to temperature changes in Dinghu and Changbai soils using the microbial inoculum originated from Dinghu (i.e., non-parallel, Fig. 4). The two functional groups displayed substantial discrepancies in terms of the magnitude and direction of their temperature responses. For example, MGE of the K-strategists under different temperatures was more stable than that of r-strategists (Fig. 4). It is intriguing to note that K_U , the half saturation constant of C uptake by microbes, K_{ED} , the half saturation constant of C degradation by extracellular enzymes, and f , the fraction of dead microbes transformed to the labile C pool, were relatively consistent among soils and microbial inoculums, particularly for K-strategists, compared to other parameters (Fig. 4).

Simulations using the constrained model shown that microbial respiration responded positively, but distinctly, to the same rate of C input among the three soils inoculated with the same microbial inoculum as well as among the three microbial inoculums inoculated to the same soil (Fig. 5). In general, microbial respiration was much more sensitive to C input changes (i.e., no C input vs C input rate of 100 $\mu\text{g C g}^{-1}$ soil C day⁻¹) under 15 °C than under 5°C. For example, in Dinghu soil inoculated with Dinghu microbial inoculum, C input had negligible effect on microbial respiration under 5 °C, but had significantly increased microbial respiration by 92 $\mu\text{g CO}_2\text{-C g}^{-1}$ SOC under 15 °C (Fig. 5a). Contrary to expectation, however, further increasing temperature from 15 °C to 25 °C did not further increase microbial respiration (Fig. 5). Indeed, C input resulted in much higher changes in microbial respiration under 15 °C than under 25 °C in Dinghu soils inoculated with Baotianman and Changbai microbial inoculums (Fig. 5a), in Baotianman soil inoculated with Baotianman microbial inoculum (Fig. 5b), and in Changbai soil inoculated with Baotianman microbial inoculum (Fig. 5c).

Discussion

Our simulation results found several interesting points regarding the temperature responses of microbial functional properties. First, most microbial properties exhibited nonlinear and non-monotonic responses to temperature. This suggests that optimal temperature may exist for microbial functioning such as MGE (which is equivalent to microbial C use efficiency), rates of uptake of labile substrates and extracellular degradation of recalcitrant C fractions. A number of empirical studies assessing the temperature sensitivity of microbial enzyme activities also have observed similar phenomenon (Hobbs *et al.* 2013; Alster *et al.* 2016b, a). For MGE, a key parameter determining the transformation of soil C, for example, its relationship with temperature is widely disputed and inconclusive; it may be positive (Manzoni *et al.* 2012; Ye *et al.* 2019), negative (Sinsabaugh *et al.* 2016), or non-monotonic (Qiao *et al.* 2019). Qiao *et al.* (2019) derived a piecewise linear function with a minimum MGE at 20 °C to model global MGE observations. Our modelling results captured such variable temperature responses. This may largely due to that an emergent microbial functional property (e.g., MGE) involves multiple microbial processes such as assimilation efficiency, biomass-specific respiration, enzyme production, and respiratory costs of enzyme production (Hagerty *et al.* 2018).

Second, microbial functional groups respond distinctly to temperature. In general, the simulation results indicated that K-strategists are more tolerant of temperature changes than r-strategists. The fast-growing r-strategists are mainly bacteria-dominated and consume labile C substrates such as sugars with fast rates, while slow-growing K-strategists are fungi-dominated and consume recalcitrant substrates such as lignin with slow rates. As such, r-strategists may be more often limited by substrate availability due to accelerated depletion of labile substrates under warming, while K-strategists are more persistent with temperature change because of slow decomposition of recalcitrant substrates. This result is consistent with empirical observations. A 12-year warming experiment in a grassland found that warming mainly impacts the activity of bacteria rather than fungi (Zhou *et al.* 2012). Laboratory incubation experiments also suggested that different prokaryotic trophic groups (e.g., copiotrophs vs oligotrophs) responded differently to changes in temperature regimes, due to distinct dynamics of soil C fractions (e.g., labile vs recalcitrant fractions) in response to temperature changes as a consequence of preferential, selective substrate utilization by microbial groups (Bai *et al.* 2017). To elucidate the mechanisms underpinning the distinct response of microbial functional

groups to temperature changes, temporal monitoring of both substrate availability with different lability and microbial community composition is required.

Third, the simulation results suggest that both historical (i.e., microbial origin) and current environments (i.e., sterilized soil and laboratory incubation) modulate microbial functioning. The importance of historical environment has been proven by results that microbial communities of different origins (i.e., soils from the three contrasting forest ecosystems) show distinct, non-parallel temperature responses when they are inoculated to the same soil (Fig. 3). This finding provides rationale for modelling the legacy effect (Jurburg *et al.* 2017; Glassman *et al.* 2018; Fukasawa *et al.* 2019). Using a reciprocal multifactorial growth chamber experiment with soil microbial communities from different origins, a recent field study also showed that soil microbial communities of different origins vary in their response to climate change factors including warming (Rasmussen *et al.* 2019). On the other hand, the same microbial community also shows distinct, non-parallel temperature responses when inoculated to different soils (Fig. 3), demonstrating the importance of current environment in regulating microbial functioning. Discrepancies in substrate quality and availability and environmental constraints between original and new environment would partially explain such phenomenon (Qin *et al.* 2019). For these reasons, microbial-mediated soil C dynamics may strongly depend on both local historical and current environmental conditions (e.g., climate, soil, and management-induced changes in soil environment) (Wu *et al.* 2010; Bradford *et al.* 2019). Indeed, these distinct, non-monotonic, and non-parallel temperature responses of microbial properties have significant consequences on microbial respiration in response to changes in C inputs (Fig. 5). This is supported by the distinct cumulative microbial respiration and their temperature responses among soil types and microbial origins in the dataset (Tang *et al.* 2018).

Conceptual C pool-based models (e.g., RothC and Century) driven by first-order kinetics are still dominant in soil C modelling. The first-order decay nature of conceptual C pools makes the conceptual C models powerless to simulate the respiration pattern in our dataset (Fig. 2), which nonetheless is normal *in situ*. For example, extreme climate events such as drought and flooding may result in marked changes in microbial growth and respiration (Lloret *et al.* 2015; Meisner *et al.* 2018). The intrinsic fluctuating nature of environment does require us to explicitly model microbial decomposition processes which may actively interact with historical and current environment, particularly in a world with more frequent extreme climate events. Microbial models have another advantage compared to conceptual C models. That is, more state variables and parameters in microbial models can be measured or reasonably estimated. In conceptual C models, almost all state variables and parameters (except total SOC content) have to be statistically fitted, e.g., the size of each C pool (because it is conceptual and thus unmeasurable) and its potential decay rate constant, resulting in large uncertainties in model predictions (Luo *et al.* 2017). Rather, a series of state variables and parameters in microbial models can be measured directly like microbial biomass and respiration, total C content, and even microbial groups with their particular functional properties, such that the uncertainties in model predictions would be reduced. For example, the result in Fig. 2 implies that another measurement of microbial biomass catching its peak may further constrain model parameters.

In conclusion, we have demonstrated that a microbial model simulating two microbial functional groups could well capture the temporal dynamics of microbial respiration. The simulation results provide novel insights into understanding microbial decomposition processes in response to warming. Microbial functional groups in terms of their substrate utilization strategies, enzyme activity, and a series of metabolic processes exhibit distinct, non-monotonic temperature responses. This may complicate the prediction of soil C dynamics in response to climatic warming. The consequences of such distinct, non-monotonic response of microbial decomposition processes on long term soil C dynamics could be substantial, and should be further verified based on long term measurements. In addition, our results demonstrated that both previous and current environments significantly shape temperature responses of microbial functional groups, resulting in that the fate of soil C under climatic warming is local soil- and climate-dependent. Above all, our data-model integration reveals that the soil-climate-microbe interactions may play a vital role in determining the fate of soil C under climatic warming, which should be properly considered in Earth system models to provide reliable predictions.

Acknowledgement

We thank funding support from the National Natural Science Foundation of China (Grand Nos. 31870426 & 31470623).

Authorship

ZL conceived and conducted the study, ZT and OJS collected the experimental data, ZL interpreted the results and wrote the manuscript with substantial contributions of all authors.

References

- Ahrens, B., Braakhekke, M.C., Guggenberger, G., Schrumpf, M. & Reichstein, M. (2015). Contribution of sorption, DOC transport and microbial interactions to the 14C age of a soil organic carbon profile: Insights from a calibrated process model. *Soil Biol. Biochem.* , 88, 390–402.
- Allison, S.D., Wallenstein, M.D. & Bradford, M.A. (2010). Soil-carbon response to warming dependent on microbial physiology. *Nat. Geosci.* , 3, 336–340.
- Alster, C.J., Baas, P., Wallenstein, M.D., Johnson, N.G. & von Fischer, J.C. (2016a). Temperature sensitivity as a microbial trait using parameters from macromolecular rate theory. *Front. Microbiol.* , 7.
- Alster, C.J., Koyama, A., Johnson, N.G., Wallenstein, M.D. & von Fischer, J.C. (2016b). Temperature sensitivity of soil microbial communities: An application of macromolecular rate theory to microbial respiration. *J. Geophys. Res. Biogeosciences* , 121, 1420–1433.
- Bai, Z., Xie, H., Kao-Kniffin, J., Chen, B., Shao, P. & Liang, C. (2017). Shifts in microbial trophic strategy explain different temperature sensitivity of CO₂ flux under constant and diurnally varying temperature regimes. *FEMS Microbiol. Ecol.* , 93.
- Bardgett, R.D., Freeman, C. & Ostle, N.J. (2008). Microbial contributions to climate change through carbon cycle feedbacks. *ISME J.*
- Bradford, M.A., McCulley, R.L., Crowther, T.W., Oldfield, E.E., Wood, S.A. & Fierer, N. (2019). Cross-biome patterns in soil microbial respiration predictable from evolutionary theory on thermal adaptation. *Nat. Ecol. Evol.* , 3, 223–231.
- Carey, J.C., Tang, J., Templer, P.H., Kroeger, K.D., Crowther, T.W., Burton, A.J., *et al.* (2016). Temperature response of soil respiration largely unaltered with experimental warming. *Proc. Natl. Acad. Sci. U. S. A.* , 113, 13797–13802.
- Chen, J., Luo, Y., García-Palacios, P., Cao, J., Dacal, M., Zhou, X., *et al.* (2018). Differential responses of carbon-degrading enzymes activities to warming: implications for soil respiration. *Glob. Chang. Biol.*
- Crowther, T.W., van den Hoogen, J., Wan, J., Mayes, M.A., Keiser, A.D., Mo, L., *et al.* (2019). The global soil community and its influence on biogeochemistry. *Science* , 365.
- Frey, S.D., Lee, J., Melillo, J.M. & Six, J. (2013). The temperature response of soil microbial efficiency and its feedback to climate. *Nat. Clim. Chang.* , 3, 395–398.
- Fukasawa, Y., Savoury, M. & Boddy, L. (2019). Ecological memory and relocation decisions in fungal mycelial networks: responses to quantity and location of new resources. *ISME J.*
- Glassman, S.I., Weihe, C., Li, J., Albright, M.B.N., Looby, C.I., Martiny, A.C., *et al.* (2018). Decomposition responses to climate depend on microbial community composition. *Proc. Natl. Acad. Sci. U. S. A.* , 115, 11994–11999.
- Hagerty, S.B., Allison, S.D. & Schimel, J.P. (2018). Evaluating soil microbial carbon use efficiency explicitly as a function of cellular processes: implications for measurements and models. *Biogeochemistry* , 140, 269–283.

Hobbs, J.K., Jiao, W., Easter, A.D., Parker, E.J., Schipper, L.A. & Arcus, V.L. (2013). Change in heat capacity for enzyme catalysis determines temperature dependence of enzyme catalyzed rates. *ACS Chem. Biol.* , 8, 2388–2393.

Jurburg, S.D., Nunes, I., Brejnrod, A., Jacquiod, S., Priemé, A., Sørensen, S.J., *et al.* (2017). Legacy effects on the recovery of soil bacterial communities from extreme temperature perturbation. *Front. Microbiol.* , 8.

Karhu, K., Auffret, M.D., Dungait, J.A.J., Hopkins, D.W., Prosser, J.I., Singh, B.K., *et al.* (2014). Temperature sensitivity of soil respiration rates enhanced by microbial community response. *Nature* .

Lloret, F., Mattana, S. & Curiel Yuste, J. (2015). Climate-induced die-off affects plant–soil–microbe ecological relationship and functioning. *FEMS Microbiol. Ecol.* , 91, 1–12.

Luo, Z., Wang, E. & Sun, O.J. (2017). Uncertain future soil carbon dynamics under global change predicted by models constrained by total carbon measurements. *Ecol. Appl.* , 27, 1001–1009.

Luo, Z., Wang, E., Zheng, H., Baldock, J. a., Sun, O.J. & Shao, Q. (2015). Convergent modeling of past soil organic carbon stocks but divergent projections. *Biogeosciences* , 12, 4245–4272.

Manzoni, S., Taylor, P., Richter, A., Porporato, A. & Ågren, G.I. (2012). Environmental and stoichiometric controls on microbial carbon-use efficiency in soils. *New Phytol.*

McGuire, K.L. & Treseder, K.K. (2010). Microbial communities and their relevance for ecosystem models: Decomposition as a case study.

Soil Biol. Biochem.

Meisner, A., Jacquiod, S., Snoek, B.L., Ten Hooven, F.C. & van der Putten, W.H. (2018). Drought legacy effects on the composition of soil fungal and prokaryote communities. *Front. Microbiol.* , 9.

Min, K., Buckeridge, K., Ziegler, S.E., Edwards, K.A., Bagchi, S. & Billings, S.A. (2019). Temperature sensitivity of biomass-specific microbial exo-enzyme activities and CO₂ efflux is resistant to change across short- and long-term timescales. *Glob. Chang. Biol.* , 25, 1793–1807.

Qiao, Y., Wang, J., Liang, G., Du, Z., Zhou, J., Zhu, C., *et al.* (2019). Global variation of soil microbial carbon-use efficiency in relation to growth temperature and substrate supply. *Sci. Rep.* , 9.

Qin, S., Chen, L., Fang, K., Zhang, Q., Wang, J., Liu, F., *et al.* (2019). Temperature sensitivity of SOM decomposition governed by aggregate protection and microbial communities. *Sci. Adv.* , 5.

Rasmussen, P.U., Bennett, A.E. & Tack, A.J.M. (2019). The impact of elevated temperature and drought on the ecology and evolution of plant–soil microbe interactions. *J. Ecol.*

Schimel, J.P. & Schaeffer, S.M. (2012). Microbial control over carbon cycling in soil. *Front. Microbiol.*

Sinsabaugh, R.L., Turner, B.L., Talbot, J.M., Waring, B.G., Powers, J.S., Kuske, C.R., *et al.* (2016). Stoichiometry of microbial carbon use efficiency in soils. *Ecol. Monogr.* , 86, 172–189.

Tang, Z., Sun, X., Luo, Z., He, N. & Sun, O.J. (2018). Effects of temperature, soil substrate, and microbial community on carbon mineralization across three climatically contrasting forest sites. *Ecol. Evol.* , 8, 879–891.

Walker, T.W.N., Kaiser, C., Strasser, F., Herbold, C.W., Leblans, N.I.W., Woebken, D., *et al.* (2018). Microbial temperature sensitivity and biomass change explain soil carbon loss with warming. *Nat. Clim. Chang.* , 1.

Wieder, W.R., Bonan, G.B. & Allison, S.D. (2013). Global soil carbon projections are improved by modelling microbial processes. *Nat. Clim. Chang.* , 3, 909–912.

Wieder, W.R., Grandy, A.S., Kallenbach, C.M. & Bonan, G.B. (2014). Integrating microbial physiology and physio-chemical principles in soils with the MICROBIAL-MINERAL CARBON STABILIZATION (MIMICS) model. *Biogeosciences* , 11, 3899–3917.

Wieder, W.R., Grandy, A.S., Kallenbach, C.M., Taylor, P.G. & Bonan, G.B. (2015). Representing life in the Earth system with soil microbial functional traits in the MIMICS model. *Geosci. Model Dev.* , 8, 1789–1808.

Wu, Y., Yu, X., Wang, H., Ding, N. & Xu, J. (2010). Does history matter? temperature effects on soil microbial biomass and community structure based on the phospholipids fatty acid (PLFA) analysis. *J. Soils Sediments* , 10, 223–230.

Ye, J.-S., Bradford, M.A., Dacal, M., Maestre, F.T. & García-Palacios, P. (2019). Increasing microbial carbon use efficiency with warming predicts soil heterotrophic respiration globally. *Glob. Chang. Biol.* , 25, 3354–3364.

Zhou, J., Xue, K., Xie, J., Deng, Y., Wu, L., Cheng, X., *et al.*(2012). Microbial mediation of carbon-cycle feedbacks to climate warming. *Nat. Clim. Chang.* , 2, 106–110.

Figure Legends

Fig. 1. Hypothesized temperature responses of microbial functional properties. For a typical microbial functional property (e.g., carbon use efficiency) of a typical microbial functional group from a typical soil, its relationship with temperature may be monotonic (**a** and **b** , i.e., the direction of the relationship does not change) or non-monotonic (**c** and **d** , i.e., the direction reverses at turning point(s)). For a typical microbial functional property (e.g., carbon use efficiency) of microbial communities from different soils, their relationship with temperature may be parallel (**a** and **c** , i.e., keep the same pace among soils) or nonparallel (**b** and **d** , i.e., do not keep the same pace among soils) among the soils.

Fig. 2. Observed and modeled microbial respiration (MR) and biomass carbon (MB). This figure shows the overall performance of the optimized model by pooling all data under all soil by microbial origin by temperature treatments. Horizontal and vertical bars show one standard deviation of observed and modeled values, respectively (5 replicates for observed, and 200 simulations for modeled). For microbial biomass carbon, there is only one measurement at the end of the experiment for model optimization (the measurement at the start of the experiment is used for model initialization). Grey dashed lines show the 1:1 line, and black solid lines show the fitted regression line. All data were natural-log transformed.

Fig. 3. Observed vs modeled temporal dynamics of microbial respiration (MR, left panels) and biomass carbon (MB, right panels). This figure shows the results in BT soil under three microbial inoculum origins (a and b, Dinghu; c and d, Baotianman; e and f, Changbai) under 15degC. Circles show the measured average, while error bars show one standard deviation ($n = 5$). Grey lines show the model predictions under 200 parameter ensembles taking into account measurement uncertainties and parameter equifinality. Please note the different scales of y axes.

Fig. 4. Temperature responses of seven microbial parameters of two functional groups of different origins and in different soils. Circles show the average and bars show its 95% confidence interval derived by conducting 200 independent optimizations taking into account measurement uncertainty and parameter equifinality. If the error bars for the same parameter are overlapped, the difference is significant. K_U and K_{ED} are normalized to the initial total soil carbon content. See Table 1 for the explanation of the seven microbial parameters.

Fig. 5. Changes in microbial respiration (MR) in response to carbon input under different temperatures . The microbial model was run for 61 days with a constant C input rate of $100 \mu\text{g C g}^{-1} \text{ soil C day}^{-1}$ using the optimized model parameters without C input. The difference of cumulative MR between simulations with and without C input was calculated (i.e., ΔMR). Error bars show the 95% confidence intervals estimated based on 200 simulations using the optimized 200 ensembles of model parameters for each soil \times microbe \times temperature combination.

Table 1. Model parameters and their prior ranges used for model optimization.

Parameter	Description	Unit	Prior range
MGE	Microbial growth efficiency	–	0.1–0.9
τ	Death rate of microbes	day ⁻¹	0–1
f	Fraction of dead microbes as labile soil C	–	0–1
$V_{\max,U}$	Maximum uptake rate of labile C by microbes	g labile C g ⁻¹ microbial C day ⁻¹	0–100
K_U	Half-saturation constant of labile C uptake by microbes	g labile C g ⁻¹ soil C	0–0.1
$V_{\max,ED}$	Maximum extracellular degradation rate of recalcitrant C	day ⁻¹	0–0.01
K_{ED}	Half-saturation constant of microbes for degradation	g microbial C g ⁻¹ soil C	0–0.1

Figure 1

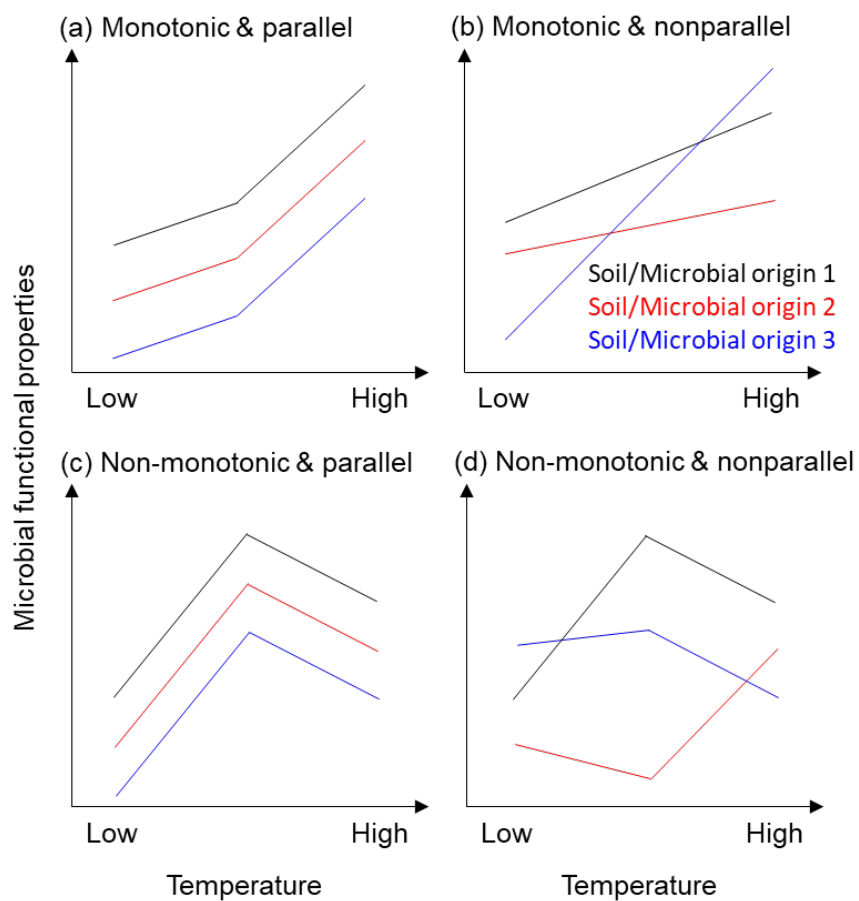


Figure 2

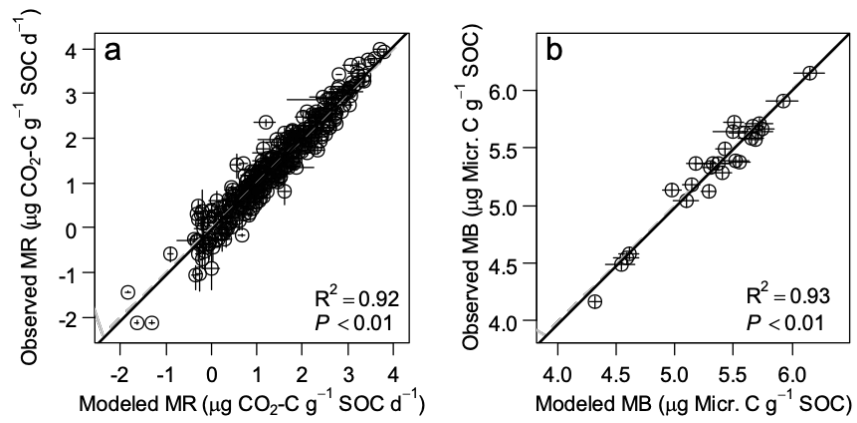


Figure 3

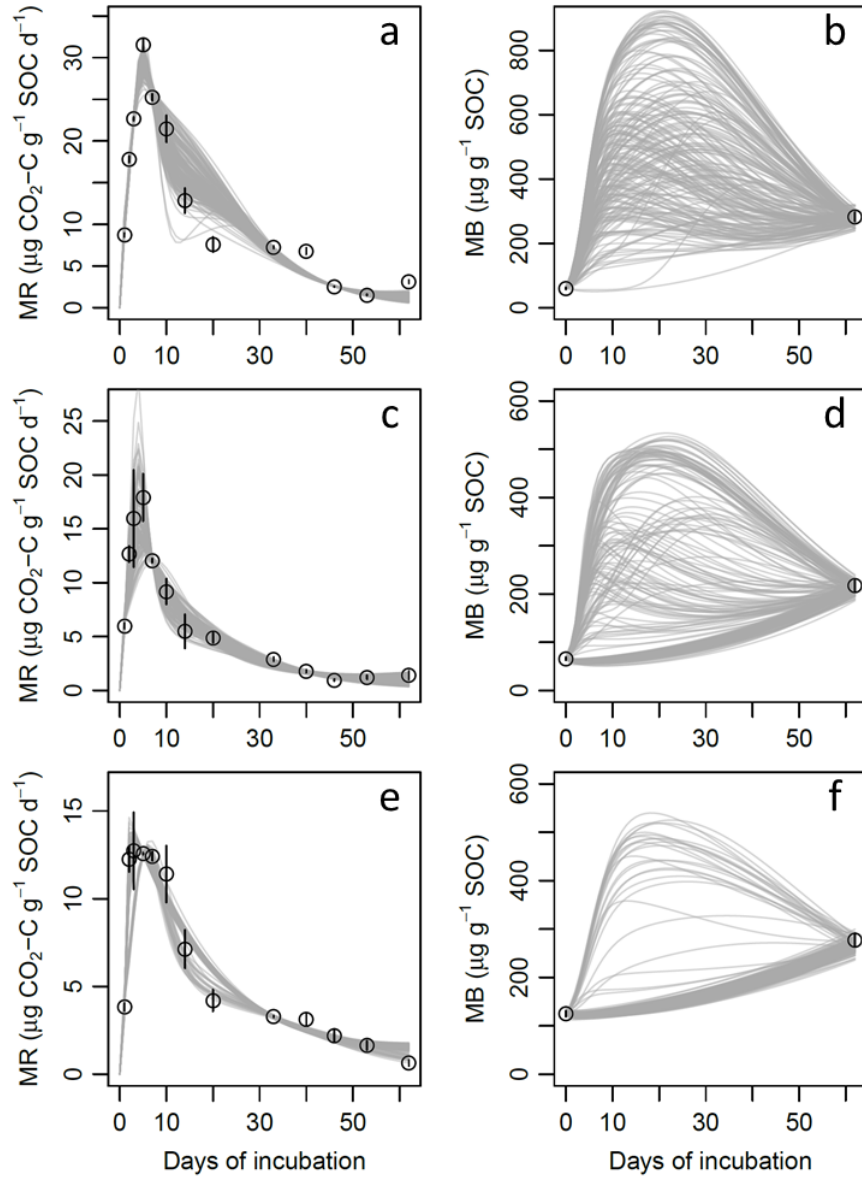


Figure 4

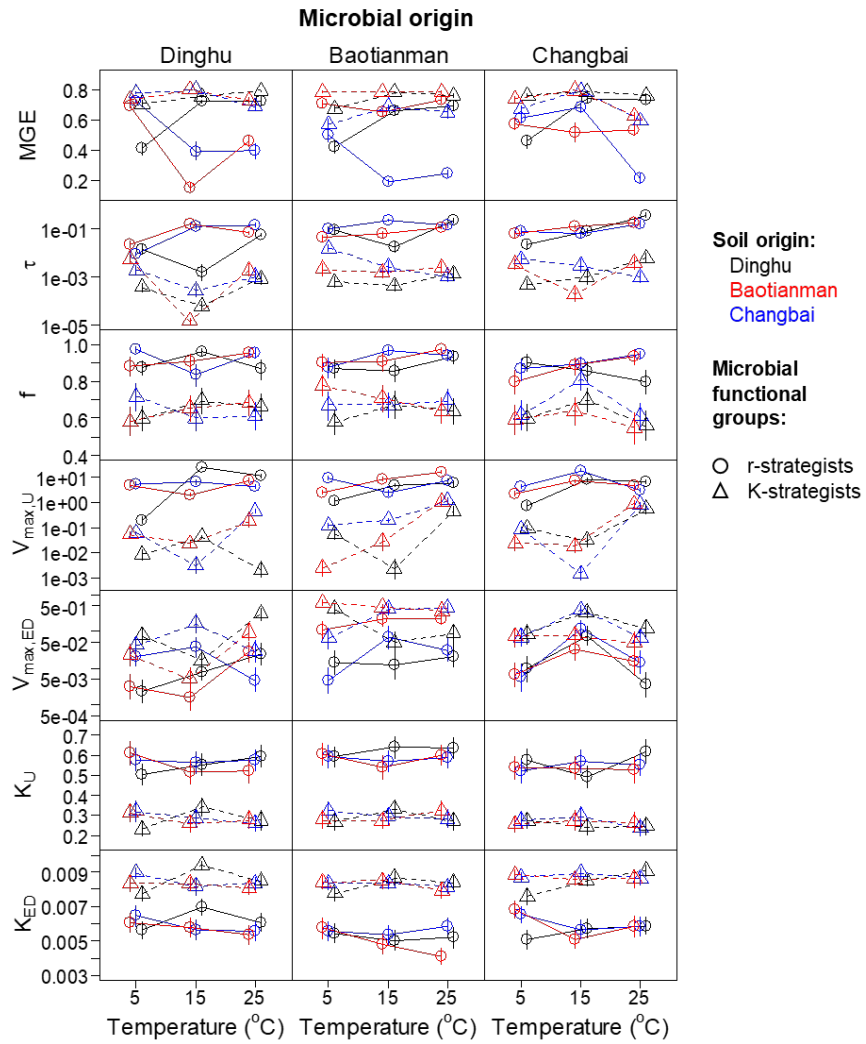


Figure 5

